

Elliptical flow coalescence to identify the $f_0(980)$ content

An Gu,^{1,*} Terrence Edmonds,^{1,†} Jie Zhao,^{1,‡} and Fuqiang Wang^{1,2,§}

¹*Department of Physics and Astronomy,*

Purdue University, West Lafayette, IN 47907, USA

²*School of Science, Huzhou University, Huzhou, Zhejiang 313000, China*

(Dated: October 18, 2021)

Abstract

We use a simple coalescence model to generate $f_0(980)$ particles for three configurations: a $s\bar{s}$ meson, a $u\bar{u}s\bar{s}$ tetraquark, and a K^+K^- molecule. The phase-space information of the coalescing constituents is taken from a multi-phase transport (AMPT) simulation of heavy-ion collisions. It is shown that the number of constituent quarks scaling of the elliptic flow anisotropy can be used to discern $s\bar{s}$ from $u\bar{u}s\bar{s}$ and K^+K^- configurations.

PACS numbers: 25.75.-q, 25.75.Ld

*Electronic address: gu180@purdue.edu

†Electronic address: tedmonds@purdue.edu

‡Electronic address: zhao656@purdue.edu

§Electronic address: fqwang@purdue.edu

I. INTRODUCTION

Exotic hadrons (hadrons with configurations other than the usual $q\bar{q}$ and $qqq(\bar{q}\bar{q}\bar{q})$ configurations) have been searched for a long time, since exotic hadron states are allowed by quantum chromodynamics (QCD) and therefore their studies can further our understanding of QCD [1]. The $f_0(980)$ is one of the candidate exotic hadrons which was first observed in $\pi\pi$ scattering experiments in the 1970's [2–4]. Its configuration is still controversial—it can be a normal $s\bar{s}$ meson, a tetraquark $s\bar{s}q\bar{q}$ state, or a $K\bar{K}$ molecule [5–7].

Heavy ion collisions create a deconfined state of quarks and gluons, called the quark-gluon plasma (QGP) [8–12]. They can provide a suitable environment to study exotic hadrons, because a large number of quarks and gluons permeate the QGP. When the temperature decreases, those quarks and gluons group into hadrons, presumably including exotic ones. The process is called hadronization process and is not well understood. A common mechanism to describe hadronization in heavy-ion collisions is the quark coalescence in which several quarks(antiquarks) combine together to form a hadron [13, 14]. Coalescence model was originally developed to describe the formation of deuterons from targets exposed to proton beams [15] and is extensively used to describe hadron production in relativistic heavy ion collisions [13, 16–19].

In non-central heavy ion collisions, the azimuthal distribution of particles is anisotropic, believed to result from hydrodynamic expansion of the initial anisotropic overlap regions [20]. The particle azimuthal distribution is often expressed in Fourier series [21]:

$$\frac{dN}{d\phi} \propto 1 + 2 \sum_{n=1}^{\infty} v_n \cos[n(\phi - \psi_n)], \quad (1)$$

where ϕ is the particle azimuthal angle, ψ_n is the n -th harmonic plane. The coefficients (v_n) are often called anisotropic flows, and are transverse momentum (p_T) and rapidity (y) dependent. In heavy-ion collisions, the leading anisotropic term is the $n = 2$ term because of the approximate elliptical shape of the collision overlap geometry; ψ_2 is a proxy for the unmeasured reaction plane and v_2 is called elliptic flow. If partons (quarks, antiquarks) which combine into a hadron have the same momentum, then we have

$$p_{T,h} = n_q \cdot p_{T,q}, \quad (2)$$

where n_q is the number of constituent quarks in the hadron. Keeping only v_2 in Eq.(1), we have

$$\begin{aligned} \frac{dN_h}{d\phi} &\propto \left(\frac{dN_q}{d\phi} \right)^{n_q} \propto [1 + 2v_{2,q}(p_{T,q}) \cos(2[\phi - \psi_{RP}])]^{n_q} \\ &\approx 1 + n_q \cdot 2v_{2,q}(p_{T,q}) \cos(2[\phi - \psi_{RP}]). \end{aligned} \quad (3)$$

Thus, we have

$$v_{2,h}(p_{T,h}) = n_q \cdot v_{2,q}(p_{T,h}/n_q). \quad (4)$$

This result is known as the number of constituent quarks (NCQ) scaling of elliptic flow, when the momenta of the coalescing (anti)quarks are not identical, the NCQ scaling is not as good [22]. Approximate NCQ scaling has been observed experimentally [23–29]. The elliptic flow of a hadron species can therefore tell us the number of constituent quarks contained in the hadron.

In this work, we use a coalescence model to study the elliptic flow (v_2) of the $f_0(980)$ for its different configuration assumptions. Although the string melting version of the AMPT model (a multiphase transport) [30] uses quark coalescence to form hadrons [31, 32], it does not produce tetraquark hadrons. In order to simulate the production of the $f_0(980)$ for different configurations, we build our own simple coalescence model. We take the phase-space information of quarks (and Kaons) from AMPT in mid-central Au+Au collisions at 200A GeV as input to our coalescence. We use this simple coalescence model to generate pions, protons, Kaons, ϕ mesons, and $f_0(980)$ particles of three configurations ($s\bar{s}$, $u\bar{u}s\bar{s}$, $K\bar{K}$) and calculate their elliptic flow. We first compare the v_2 of pions and protons from our coalescence model with those from AMPT to validate our simple coalescence model approach. We then study the NCQ scaling of the $f_0(980)$ v_2 and demonstrate that it is a viable way to identify its quark content.

II. COALESCENCE MODEL

The main idea of the coalescence model is to combine several partons into one hadron. The model was implemented in heavy ion collisions to describe the NCQ scaling of elliptic flow, the baryon-to-meson ratio, and the hadron transverse momentum spectra, which can not be described well by fragmentation model [17].

Suppose N constituent particles are coalesced into a composite particle (a hadron or a $K\bar{K}$ molecule). The total yield of the composite particle can be expressed as [13]

$$N_c = g_c \int \left(\prod_{i=1}^N dN_i \right) f_c^W(\vec{r}_1, \dots, \vec{r}_N, \vec{p}_1, \dots, \vec{p}_N). \quad (5)$$

Here $f_c^W(\vec{r}_1, \dots, \vec{r}_N, \vec{p}_1, \dots, \vec{p}_N)$ is the Wigner function (WF) which is proportional to the coalescence probability and g_c is a statistical factor. The statistical factor g_c only affects the yield of the hadrons instead of the elliptic flow, so we set $g_c = 1$ for all kinds of hadrons in this study.

For a meson, if two quarks form a harmonic oscillator and they are in s-state, then the WF is Gaussian [33]:

$$f_{meson}(\vec{r}_1, \vec{r}_2, \vec{p}_1, \vec{p}_2) = A \cdot \exp \left(-\frac{r_{12}^2}{\sigma_r^2} - \frac{p_{12}^2}{\sigma_p^2} \right), \quad (6)$$

where

$$r_{ij}^2 = (\vec{r}_i - \vec{r}_j)^2, \quad p_{ij}^2 = (\vec{p}_i - \vec{p}_j)^2. \quad (7)$$

Here, \vec{r}_i and \vec{p}_i are the position and momentum of i -th quark/antiquark at the time the hadron is formed. In AMPT, partons freeze out (FO, which means this (anti)quark doesn't interact with others anymore) at different times t_i . The moment for two or more (anti)quarks to coalesce is set to be the latest freeze out time of those (anti)quarks, t_F . The final positions are calculated as $\vec{r}_i = \vec{r}_{i,FO} + \vec{v}_{i,FO} \times (t_F - t_{i,FO})$. For K and \bar{K} particles, we take their FO phase space information right after they are formed in AMPT.

There are two parameters in Eq.(6), A and σ_r ($\sigma_p = 1/\sigma_r$). The parameter $A \leq 1$ only affects the total yield of hadrons, not the v_2 , so we set it to 1. Assuming the system is in s-wave state, we have $\sigma_r = 1/\sqrt{\mu\omega}$, where μ is the reduced mass of the two-body system, and ω is the oscillator frequency. The oscillator frequency can be fixed by $\omega = 3/(2\mu_1\langle r^2 \rangle)$, where $\langle r^2 \rangle$ is the mean square radius of the hadron [33]. Thus, we have $\sigma_r = \sqrt{2\langle r^2 \rangle/3}$. For pions, $\langle r^2 \rangle = (0.61 \pm 0.15) \text{ fm}^2$ [34], so we set $\sigma_r = 0.64 \text{ fm}$. For kaons, $\langle r^2 \rangle = (0.34 \pm 0.05) \text{ fm}^2$ [35], we set $\sigma_r = 0.48 \text{ fm}$. For phi mesons ($s\bar{s}$), its internal structure and radius is still not well known, and its cross section with nonstrange hadron is small [36], so we set $\sigma_r = 0.5 \text{ fm}$.

For multi-particle systems, the quantum state is difficult to compute analytically. For tetraquark and pentaquark hadrons, only the heavy quark sector has been calculated quantum mechanically using perturbative approaches [37–40]. In this work, for baryons and tetraquark systems, we naively define the Wigner function also to be Gaussian. For baryons,

$$f_{baryon}(\vec{r}_1, \vec{r}_2, \vec{r}_3, \vec{p}_1, \vec{p}_2, \vec{p}_3) = A \cdot \exp \left(-\frac{1}{3\sigma_r^2} \cdot \sum_{i,j=1}^3 \sum_{i<j} r_{ij}^2 - \frac{1}{3\sigma_p^2} \cdot \sum_{i,j=1}^3 \sum_{i<j} p_{ij}^2 \right), \quad (8)$$

and for tetraquarks,

$$f_{tetra}(\vec{r}_1, \vec{r}_2, \vec{r}_3, \vec{r}_4, \vec{p}_1, \vec{p}_2, \vec{p}_3, \vec{p}_4) = A \cdot \exp \left(-\frac{1}{6\sigma_r^2} \cdot \sum_{i,j=1}^4 \sum_{i<j} r_{ij}^2 - \frac{1}{6\sigma_p^2} \cdot \sum_{i,j=1}^4 \sum_{i<j} p_{ij}^2 \right). \quad (9)$$

For protons, $\sqrt{\langle r^2 \rangle} = 0.88 \text{ fm}$ [41], so we set $\sigma_r = \sqrt{2\langle r^2 \rangle/3} = 0.72 \text{ fm}$. For the $f_0(980)$ particles, we have $\omega = 67.8 \text{ MeV}$ [42]. If we consider $s\bar{s}$ configuration, the reduced mass is $\mu = m_s/2$ with $m_s = 0.199 \text{ GeV}/c^2$ [30], so $\sigma_r = 1/\sqrt{\mu\omega} = 2.4 \text{ fm}$. We set this value of σ_r for all three different configurations of the $f_0(980)$. In our coalescence model, we get the freeze out information of (anti)quarks after the parton cascade in AMPT. We input this information to our simple coalescence model to produce hadrons. We loop over all available (anti)quarks to form pions, protons, or $f_0(980)$, and we carry out the coalescence separately for each of these species. For each species, if the flavors of the (anti)quarks are correct for the hadron and the value of a random number (uniformly distributed between 0 and 1) is smaller than the value of the Wigner function, the hadron is formed. The four momentum of the hadron is calculated as the sum of the four momentum of its constituents, $p_h^\mu = \sum_i p_{q,i}^\mu$. And these (anti)quarks are then removed from further consideration of coalescence.

III. RESULTS

We use this simple coalescence model to generate pions, protons, Kaons, ϕ mesons, and $f_0(980)$ of three different configurations ($s\bar{s}$, $u\bar{u}s\bar{s}$, K^+K^-).

In each event, the elliptic flow v_2 [43, 44] is calculated as:

$$v_2 = \left\langle \cos 2(\phi - \psi_2^{(r)}) \right\rangle. \quad (10)$$

Here $\psi_2^{(r)}$ is the 2nd harmonic plane of each event in the spatial configuration space of the initial overlap geometry, and is obtained by

$$\psi_2^{(r)} = [\text{atan2}(\langle r_\perp^2 \sin 2\phi_r \rangle, \langle r_\perp^2 \cos 2\phi_r \rangle) + \pi] / 2, \quad (11)$$

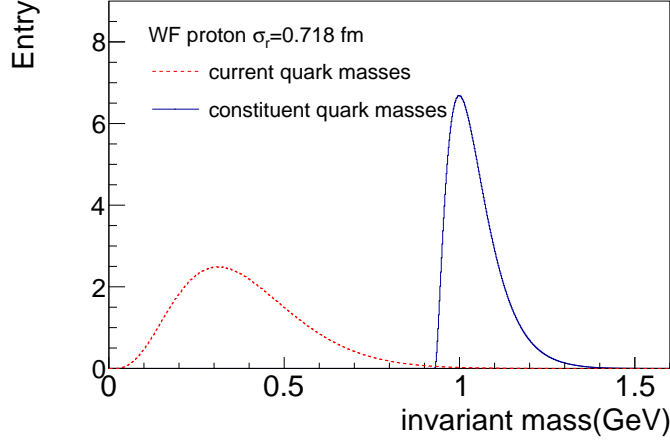


FIG. 1: Invariant mass spectra of protons from our Gaussian-WF coalescence with current quark masses (as in AMPT) and constituent quark masses, respectively.

where r_{\perp} and ϕ_r are the polar coordinate of each initial parton before the parton cascade [45]. The resolution of $\psi_2^{(r)}$ is close to 1 due to the large initial parton multiplicity [44]. The elliptic flow shown in this study are for particles within pseudo-rapidity window $|\eta| < 1$.

We first compare the results of pions and protons from our coalescence model with those from AMPT. We then present the $f_0(980)$ results from our coalescence model.

A. Proton and Pion

The quark masses used in our study are from the AMPT model (the same as PYTHIA program [30]). It would be more reasonable to use the constituent quark masses [46] to take into account the effects of gluons, but as we show below, the quark masses do not significantly alter our results, so we stick to the masses used in the AMPT model.

Figure 1 shows the mass spectra of protons from our Gaussian-WF coalescence with AMPT quark masses (red line) and constituent quark masses (blue line) ($m_u = m_d = 0.31$ GeV [46]). We can see that the coalescence model does not generate correct mass spectra, which is a well-known problem [30, 32].

Figure 2 shows v_2/n_q vs. p_T/n_q for the pions (blue circle, $n_q = 2$) and protons (red square, $n_q = 3$) from our Gaussian-WF coalescence compared to those from AMPT model (blue line and red line). The pions from the Gaussian-WF coalescence have similar v_2/n_q to pions from AMPT at low p_T and lower v_2/n_q than AMPT pions at high p_T/n_q . While the WF

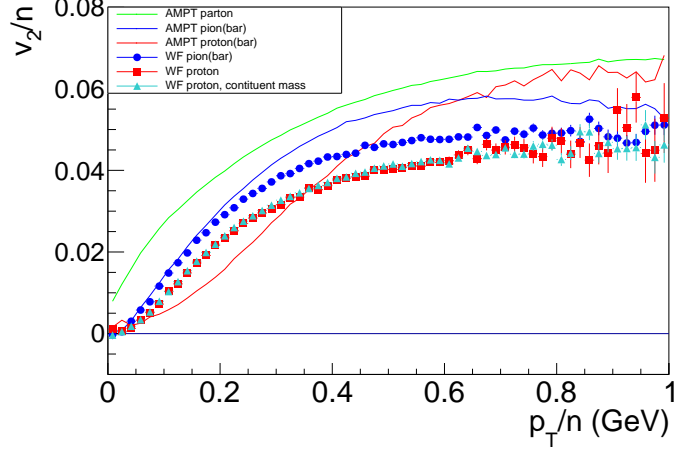


FIG. 2: v_2/n_q vs. p_T/n_q of pions and protons from Gaussian-WF coalescence compared to those from AMPT.

protons have higher v_2/n_q than AMPT protons at low p_T but lower v_2/n_q at high p_T/n_q .

We checked whether the masses of quarks would affect the v_2/n_q vs. p_T/n_q by using constituent quark masses in coalescence. To do that, we simply take the AMPT quark freezeout momenta and recalculate their velocity using constituent quark masses in propagation of quarks from freeze out to coalescence point. The result is shown in Fig. 2 where v_2/n_q vs. p_T/n_q of protons generated from our coalescence with constituent quark masses (light blue triangle) is also presented. The masses of quarks have practically no effect on the v_2/n_q . This is expected because in our simple coalescence model, the masses of quarks only affect the speeds of quarks (most relativistic), which are only related to the final spatial position of the quarks. While the v_2 only depends on the momentum of quarks, so the v_2 would be almost independent of the quark masses.

We apply invariant mass cut on protons and pions from our Gaussian-WF coalescence as shown in Fig.3. Generally, hadrons with larger invariant masses have less v_2 since their constituent quarks are farther away from each other in momentum space. When $\text{mass} < 0.2$ GeV is applied to pions and $\text{mass} > 0.4$ GeV is applied to protons from the Gaussian-WF coalescence, our simple coalescence model gives more consistent results with those from the coalescence model used in the AMPT. This is understandable because the invariant mass is utilized by AMPT to assign hadrons [30]. It is also an indication that our simple coalescence model is doing a reasonable job.

As mentioned in the introduction, the NCQ scaling is best satisfied when the coalescing

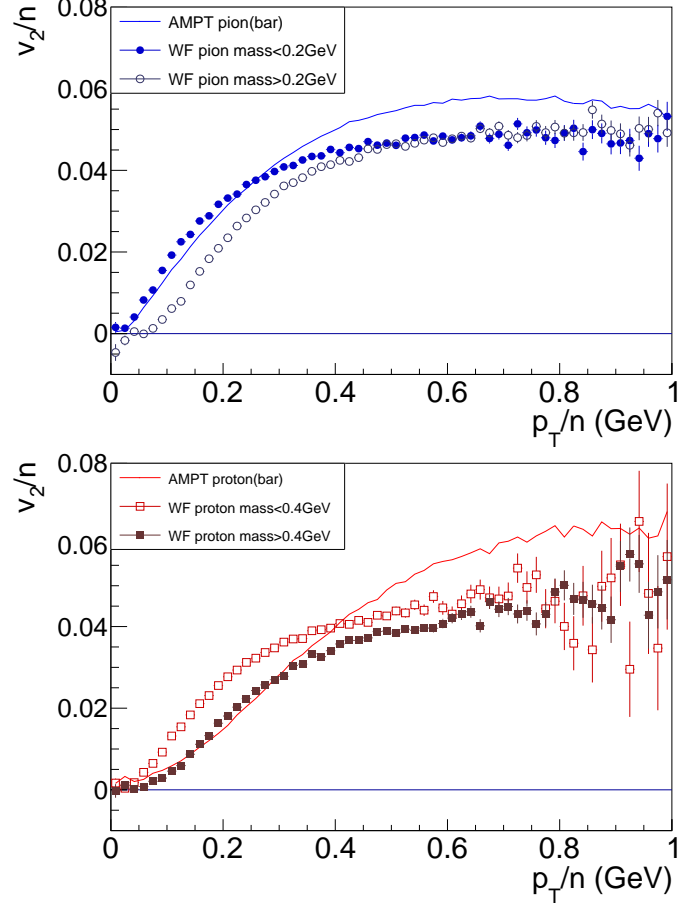


FIG. 3: v_2/n_q vs. p_T/n_q of pions (upper) and protons (lower) from Gaussian-WF coalescence for different mass cuts, compared to AMPT results.

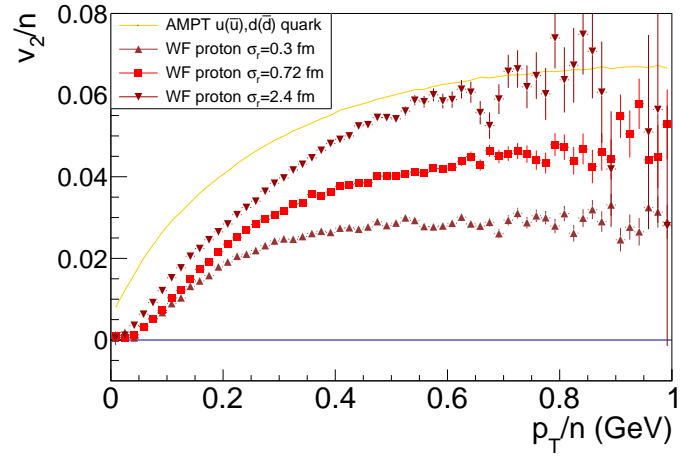


FIG. 4: v_2/n_q vs. p_T/n_q of protons generated with different values of σ_r from our WF-Gaussian coalescence, compared to that of light quarks from AMPT.

partons have the same momentum. When their momenta differ, the NCQ will not be as good. Since the smaller the σ_r the larger their momentum difference ($\sigma_p = 1/\sigma_r$), we expect the goodness of the NCQ scaling to increase with σ_r . Thus we artificially change the σ_r of the proton and check how the proton v_2/n_q vs. p_T/n_q changes relative to the light quark v_2 . This is shown in Fig. 4. Indeed, we observe that protons with larger value of σ_r have closer v_2/n_q vs. p_T/n_q to that of the $u(\bar{u}), d(\bar{d})$ quarks, i.e. closer to the ideal situation of NCQ scaling of elliptic flow ($\sigma_p \rightarrow 0$). Likewise it is reasonable for the pions and protons to have different v_2/n_q vs. p_T/n_q from the quarks as shown in Fig. 2 because of the relatively small values of σ_r .

It is interesting to notice that although protons are generated with larger σ_r ($\sigma_r = 0.72$ fm) than the pions ($\sigma_r = 0.64$ fm), the $v_2/n_q(p_T/n_q)$ of protons is lower than that of pions. This is because there are more constituent quarks in a parton than a pion. So there is a larger reduction in v_2 from the ideal NCQ scaling picture. That is to say, in our Gauss-WF coalescence model, hadrons containing more constituents will have lower $v_2/n_q(p_T/n_q)$ for a given limited value of σ_r .

B. $f_0(980)$ particle for three configurations($s\bar{s}, u\bar{u}s\bar{s}, K^+K^-$)

Figure 5 shows v_2/n_q vs. p_T/n_q ($n_q=4$) for the tetraquark state of $f_0(980)$ from our Gaussian-WF coalescence for different mass cuts. The mass spectrum of $f_0(980)$ in tetraquark state from our Gaussian-WF coalescence is shown in the insert. The mass spectrum of $f_0(980)$ does not peak at 980 MeV. Using larger constituent quark masses could improve the situation. Similar to the protons shown in Fig.3, the mass cut does not significantly change the v_2/n_q of $f_0(980)$ either.

For comparison, the v_2 vs. p_T of light quark and strange quark from AMPT are also shown in Fig.5. It is interesting to note that the $v_2/n_q(p_T/n_q)$ of the $f_0(980)(u\bar{u}s\bar{s})$ is lower than those of u-quarks and s-quarks, whereas one would naively expect the the $f_0(980)(u\bar{u}s\bar{s})$ results to be midway between u-quarks and s-quarks curves. In the ideal NCQ scaling picture, all the coalesced quarks in the hadron possess the same momentum, i.e. $\sigma_p \rightarrow 0$ and $\sigma_r \rightarrow \infty$. Hence the v_2/n_q of $f_0(u\bar{u}s\bar{s})$ should be $(v_{2,u\bar{u}} + v_{2,s\bar{s}})/2$ because:

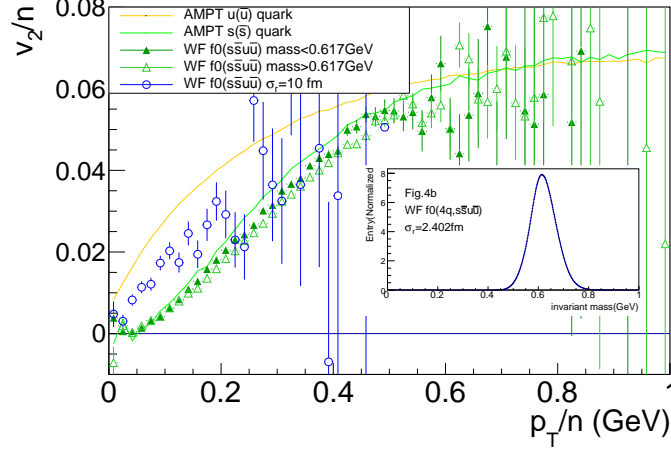


FIG. 5: v_2/n_q vs. p_T/n_q , for the tetraquark state of $f_0(980)$ from our Gaussian-WF coalescence ($\sigma_r = 2.4$) fm for different mass cuts. For comparison, the $f_0(980)$ results with $\sigma_r = 10$ fm are also shown. The curves show the results of light and strange quarks from AMPT.

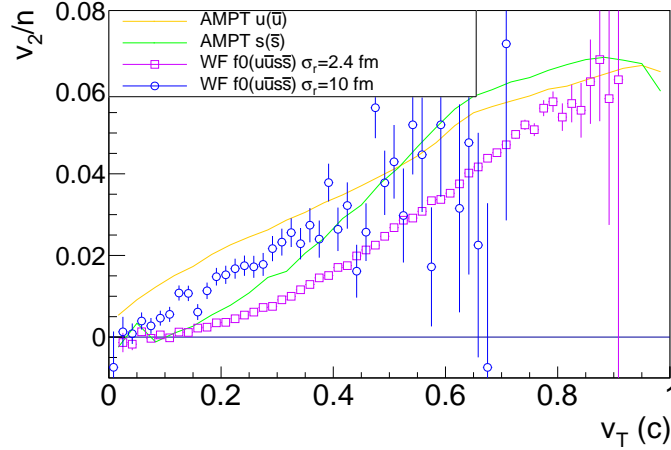


FIG. 6: v_2/n_q vs. v_T , for the tetraquark state of $f_0(980)$ from our Gaussian-WF coalescence for constituent quark masses and different values of σ_r . The curves are the results of up quark and strong quark from AMPT calculated by using constituent quark masses.

$$\begin{aligned} \frac{dN_{f_0(980)(u\bar{u}s\bar{s})}}{d\phi} &\propto [1 + 2v_{2,u}(p_{T,u}) \cos(2[\phi - \psi_{RP}])]^2 \cdot [1 + 2v_{2,s}(p_{T,s}) \cos(2[\phi - \psi_{RP}])]^2 \quad (12) \\ &\approx 1 + 2 \cdot [2v_{2,u}(p_{T,f_0(980)}/4) + 2v_{2,s}(p_{T,f_0(980)}/4)] \cos(2[\phi - \psi_{RP}]). \end{aligned}$$

To test this, we artificially set σ_r to a large value ($\sigma_r = 10$ fm) to mimic the ideal NCQ scaling picture. The results are shown in Fig.5 as the blue open circles. Indeed, the $v_2(p_T/n_q)$ of the $f_0(u\bar{u}s\bar{s})$ lies midway between those of u-quarks and s-quarks as expected in the ideal

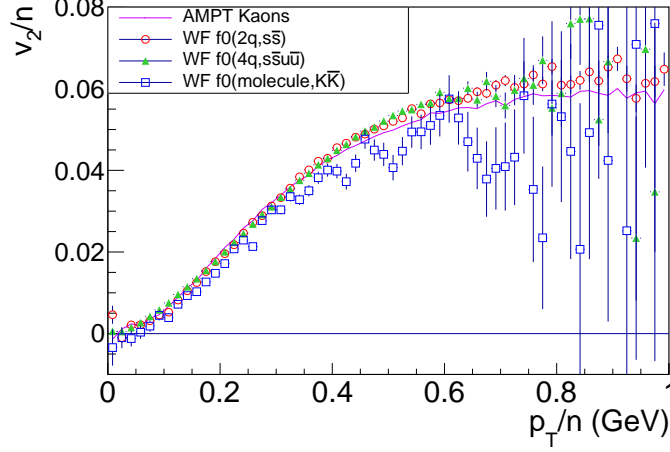


FIG. 7: v_2/n_q vs. p_T/n_q for different configurations of $f_0(980)$ from our Gaussian-WF coalescence compared to the Kaon result from AMPT.

picture.

In the coalescence, one often considers the velocities of the constituents. In order to examine the elliptic flow as a function of velocity, we use the large constituent quark masses ($m_u = 0.31$ GeV, $m_s = 0.5$ GeV) to produce the $f_0(980)(u\bar{u}s\bar{s})$. Similar to the protons, the $v_2/n_q(p_T/n_q)$ of $f_0(980)(u\bar{u}s\bar{s})$ using constituent quark masses is almost as same as that using constituent quark masses. The v_2/n_q of $f_0(980)(u\bar{u}s\bar{s})$ as a function of transverse velocity v_T is shown in Fig.6 together with those of constituent u-quarks and s-quarks. When σ_r of $f_0(980)(u\bar{u}s\bar{s})$ is set to 10 fm, the $v_2/n_q(v_T)$ also lies midway between those of u-quarks and s-quarks as expected in the ideal picture. The $v_2/n_q(v_T)$ is qualitatively similar to the $v_2/n_q(p_T/n_q)$ shown in Fig.5. This is because the constituent masses of u-quarks and s-quarks are not very different. It should be noted, however, that in our Gauss-WF coalescence model, it is the momentum, not the velocity that is used to calculate the coalescence probability. Hence, the momentum is the more relevant variable to use than the velocity.

The above results indicate that our coalescence model is doing a reasonable job to produce tetraquark hadrons. In the following, we use our coalescence model to produce the $f_0(980)$ of the other two configurations ($s\bar{s}$ and $K\bar{K}$) and compare the elliptic flows of these three configurations.

In Fig.7, we compare v_2/n_q vs. p_T/n_q of different configurations of $f_0(980)$. The v_2/n_q is almost the same for different configurations ($s\bar{s}$, $u\bar{u}s\bar{s}$, K^+K^-). It is easy to understand why $f_0(980)(K^+K^-)$ ($n_q = 4$) has the same $v_2/n_q(p_T/n_q)$ as the $f_0(980)(s\bar{s})$ ($n_q = 2$). This

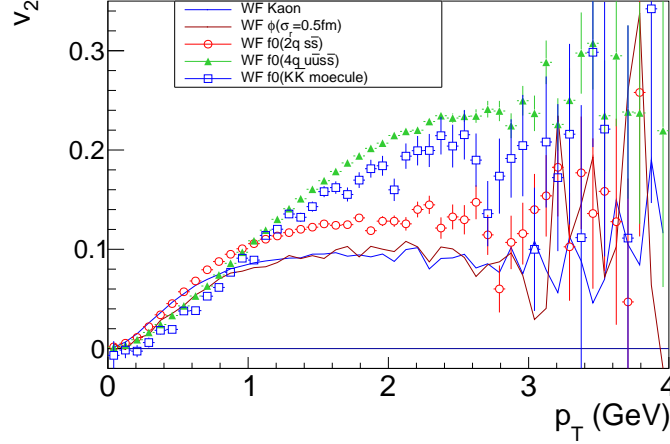


FIG. 8: v_2 vs. p_T , for Kaons, ϕ , and three different configurations of $f_0(980)$ from our Gaussian-WF coalescence model.

is because they are both from the two-body coalescence with the same value of σ_r , and because in AMPT kaons ($n_q = 2$) have almost the same $v_2/n_q(p_T/n_q)$ as that of the strange quarks ($n_q = 1$).

However, it is somewhat surprising that the $v_2/n_q(p_T/n_q)$ of $f_0(u\bar{u}s\bar{s})$ is almost the same as that of $f_0(s\bar{s})$. As we have previously pointed out that in our Gauss-WF coalescence model, for a given value of σ_r , hadrons containing more constituents will have lower $v_2/n_q(p_T/n_q)$. Thus we would expect the $v_2/n_q(p_T/n_q)$ of $f_0(u\bar{u}s\bar{s})$ to be lower than that of the $f_0(s\bar{s})$, which is not true here. This is because of another effect, i.e. the u-quarks that $f_0(u\bar{u}s\bar{s})$ contains have larger $v_2/n_q(p_T/n_q)$ and upraise that of the $f_0(u\bar{u}s\bar{s})$. As a result, the $f_0(980)$ of $u\bar{u}s\bar{s}$ and $s\bar{s}$ configurations happen to have almost the same $v_2/n_q(p_T/n_q)$.

The common dependence of the v_2/n_q vs. p_T/n_q in Fig.7 indicates that the NCQ scaling of $f_0(980)$ can be used to tell its number of constituent quarks. This is more evidently shown in Fig.8 where the v_2 is directly shown as a function of p_T . The $v_2(p_T)$ of $f_0(980)$ with $(s\bar{s})$ configuration is very different from the other configurations, especially when $p_T > 1$ GeV. So according to our simple coalescence model, experimental measurement of v_2 can tell whether f_0 particle is composed of 2 quarks. It is however difficult to tell the difference between the 4-quark configuration and K^+K^- molecule configuration. This is not surprising because the K^+K^- molecule is effectively a “four-quark” state.

Studying the yield of exotic hadrons in heavy ion collisions using coalescence model is another way to discriminate between different configurations. It is shown that the yield

of an exotic hadron (such as a tetraquark state) is significantly smaller than the yield of a non-exotic hadron with normal number of constituent quarks [42]. This can be used to further separate tetraquark $f_0(980)$ from a K^+K^- molecule state.

IV. CONCLUSION

We used a simple coalescence model with Gaussian Wigner function to generate pions, protons, kaons, ϕ mesons, and $f_0(980)$ particles of three different configurations ($s\bar{s}$, $u\bar{u}s\bar{s}$, K^+K^-). The NCQ scaling of elliptic flow v_2 is observed in our study, and can be used to distinguish the $s\bar{s}$ state of the $f_0(980)$ from the tetraquark ($u\bar{u}s\bar{s}$) or K^+K^- molecule state in heavy ion collisions. It is difficult to tell apart the $u\bar{u}s\bar{s}$ and K^+K^- states by measuring v_2 . The $f_0(980)$ yields needs to be exploited.

Acknowledgement

We thank Dr. Pengfei Zhuang and Dr. Zi-wei Lin for fruitful discussions. This work was supported in part by the U.S. Department of Energy (Grant No. de-sc0012910) and the National Natural Science Foundation of China (Grant No. 11747312).

-
- [1] R. L. Jaffe. Exotica. *Phys. Rept.*, 409:1–45, 2005. [191(2004)].
 - [2] S. D. Protopopescu, M. Alston-Garnjost, A. Barbaro-Galtieri, Stanley M. Flatte, J. H. Friedman, T. A. Lasinski, G. R. Lynch, M. S. Rabin, and F. T. Solmitz. Pi pi Partial Wave Analysis from Reactions $\pi^+ p \rightarrow \pi^+ \pi^- \Delta^{++}$ and $\pi^+ p \rightarrow \pi^+ \pi^- K^+ K^- \Delta^{++}$ at 7.1-GeV/c. *Phys. Rev.*, D7:1279, 1973.
 - [3] B. Hyams et al. $\pi\pi$ Phase Shift Analysis from 600-MeV to 1900-MeV. *Nucl. Phys.*, B64:134–162, 1973.
 - [4] G. Grayer et al. High Statistics Study of the Reaction $\pi^- p \rightarrow \pi^- \pi^+ n$: Apparatus, Method of Analysis, and General Features of Results at 17-GeV/c. *Nucl. Phys.*, B75:189–245, 1974.
 - [5] D. V. Bugg. Four sorts of meson. *Phys. Rept.*, 397:257–358, 2004.
 - [6] Eberhard Klempt and Alexander Zaitsev. Glueballs, Hybrids, Multiquarks. Experimental facts versus QCD inspired concepts. *Phys. Rept.*, 454:1–202, 2007.
 - [7] J. R. Pelaez. From controversy to precision on the sigma meson: a review on the status of the non-ordinary $f_0(500)$ resonance. *Phys. Rept.*, 658:1, 2016.
 - [8] K. Adcox et al. Formation of dense partonic matter in relativistic nucleus-nucleus collisions at RHIC: Experimental evaluation by the PHENIX collaboration. *Nucl. Phys.*, A757:184–283, 2005.
 - [9] I. Arsene et al. Quark gluon plasma and color glass condensate at RHIC? The Perspective from the BRAHMS experiment. *Nucl. Phys.*, A757:1–27, 2005.
 - [10] B. B. Back et al. The PHOBOS perspective on discoveries at RHIC. *Nucl. Phys.*, A757:28–101, 2005.
 - [11] John Adams et al. Experimental and theoretical challenges in the search for the quark gluon plasma: The STAR Collaboration’s critical assessment of the evidence from RHIC collisions. *Nucl. Phys.*, A757:102–183, 2005.
 - [12] Berndt Muller, Jurgen Schukraft, and Boleslaw Wyslouch. First Results from Pb+Pb collisions at the LHC. *Ann. Rev. Nucl. Part. Sci.*, 62:361–386, 2012.
 - [13] Carl B. Dover, Ulrich W. Heinz, Ekkard Schnedermann, and Jozsef Zimanyi. Relativistic coalescence model for high-energy nuclear collisions. *Phys. Rev.*, C44:1636–1654, 1991.
 - [14] Rainer J. Fries, Vincenzo Greco, and Paul Sorensen. Coalescence Models For Hadron Forma-

- tion From Quark Gluon Plasma. *Ann.Rev.Nucl.Part.Sci.*, 58:177–205, 2008.
- [15] S. T. Butler and C. A. Pearson. Deuterons from High-Energy Proton Bombardment of Matter. *Phys. Rev.*, 129:836–842, 1963.
 - [16] R. J. Fries, Berndt Muller, C. Nonaka, and S. A. Bass. Hadronization in heavy ion collisions: Recombination and fragmentation of partons. *Phys. Rev. Lett.*, 90:202303, 2003.
 - [17] R. J. Fries, Berndt Muller, C. Nonaka, and S. A. Bass. Hadron production in heavy ion collisions: Fragmentation and recombination from a dense parton phase. *Phys. Rev.*, C68:044902, 2003.
 - [18] V. Greco, C. M. Ko, and P. Levai. Parton coalescence at RHIC. *Phys. Rev.*, C68:034904, 2003.
 - [19] Vincenzo Minissale, Francesco Scardina, and Vincenzo Greco. Hadrons from coalescence plus fragmentation in AA collisions at energies available at the BNL Relativistic Heavy Ion Collider to the CERN Large Hadron Collider. *Phys. Rev.*, C92(5):054904, 2015.
 - [20] Jean-Yves Ollitrault. Anisotropy as a signature of transverse collective flow. *Phys.Rev.*, D46:229–245, 1992.
 - [21] S. Voloshin and Y. Zhang. Flow study in relativistic nuclear collisions by Fourier expansion of Azimuthal particle distributions. *Z. Phys.*, C70:665–672, 1996.
 - [22] Denes Molnar and Sergei A. Voloshin. Elliptic flow at large transverse momenta from quark coalescence. *Phys.Rev.Lett.*, 91:092301, 2003.
 - [23] John Adams et al. Particle type dependence of azimuthal anisotropy and nuclear modification of particle production in Au + Au collisions at $s(\text{NN})^{1/2} = 200\text{-GeV}$. *Phys. Rev. Lett.*, 92:052302, 2004.
 - [24] J. Adams et al. Azimuthal anisotropy in Au+Au collisions at $s(\text{NN})^{1/2} = 200\text{-GeV}$. *Phys. Rev.*, C72:014904, 2005.
 - [25] J. Adams et al. Multi-strange baryon elliptic flow in Au + Au collisions at $s(\text{NN})^{1/2} = 200\text{-GeV}$. *Phys. Rev. Lett.*, 95:122301, 2005.
 - [26] A. Adare et al. Scaling properties of azimuthal anisotropy in Au+Au and Cu+Cu collisions at $s(\text{NN}) = 200\text{-GeV}$. *Phys. Rev. Lett.*, 98:162301, 2007.
 - [27] B. I. Abelev et al. Partonic flow and phi-meson production in Au + Au collisions at $s(\text{NN})^{1/2} = 200\text{-GeV}$. *Phys. Rev. Lett.*, 99:112301, 2007.
 - [28] L. Adamczyk et al. Elliptic flow of identified hadrons in Au+Au collisions at $\sqrt{s_{\text{NN}}} = 7.7\text{-}62.4$

- GeV. *Phys. Rev.*, C88:014902, 2013.
- [29] Betty Bezverkhny Abelev et al. Elliptic flow of identified hadrons in Pb-Pb collisions at $\sqrt{s_{\text{NN}}} = 2.76$ TeV. *JHEP*, 06:190, 2015.
 - [30] Zi-Wei Lin, Che Ming Ko, Bao-An Li, Bin Zhang, and Subrata Pal. A Multi-phase transport model for relativistic heavy ion collisions. *Phys. Rev.*, C72:064901, 2005.
 - [31] Zi-wei Lin and Denes Molnar. Quark coalescence and elliptic flow of charm hadrons. *Phys. Rev.*, C68:044901, 2003.
 - [32] Yuncun He and Zi-Wei Lin. Improved Quark Coalescence for a Multi-Phase Transport Model. *Phys. Rev.*, C96(1):014910, 2017.
 - [33] A. J. Baltz and C. Dover. Quark model of phi coalescence from kaons in heavy ion reactions. *Phys. Rev.*, C53:362–366, 1996.
 - [34] G.T. Adylov, F.K. Aliev, D.Yu. Bardin, W. Gajewski, I. Ion, B.A. Kulakov, G.V. Micelmacher, B. Niczyporuk, T.S. Nigmanov, E.N. Tsyganov, M. Turala, A.S. Vodopianov, K. Wala, E. Dally, D. Drickey, A. Liberman, P. Shepard, J. Tompkins, C. Buchanan, and J. Poirier. The pion radius. *Physics Letters B*, 51(4):402 – 406, 1974.
 - [35] S. R. Amendolia et al. A Measurement of the Kaon Charge Radius. *Phys. Lett.*, B178:435–440, 1986.
 - [36] A. Shor. Phi Meson Production as a Probe of the Quark Gluon Plasma. *Phys. Rev. Lett.*, 54:1122–1125, 1985.
 - [37] Ahmed Ali, Jens Sren Lange, and Sheldon Stone. Exotics: Heavy Pentaquarks and Tetraquarks. *Prog. Part. Nucl. Phys.*, 97:123–198, 2017.
 - [38] Hua-Xing Chen, Wei Chen, Xiang Liu, and Shi-Lin Zhu. The hidden-charm pentaquark and tetraquark states. *Phys. Rept.*, 639:1–121, 2016.
 - [39] D. M. Brink and Fl. Stancu. Tetraquarks with heavy flavors. *Phys. Rev. D*, 57:6778–6787, Jun 1998.
 - [40] Shuzhe Shi, Xingyu Guo, and Pengfei Zhuang. Flavor Dependence of Meson Melting Temperature in Relativistic Potential Model. *Phys. Rev.*, D88(1):014021, 2013.
 - [41] A Antognini, F D Amaro, F Biraben, J M R Cardoso, D S Covita, A Dax, S Dhawan, L M P Fernandes, A Giesen, T Graf, T W Hnsch, P Indelicato, L Julien, C Y Kao, P Knowles, F Kottmann, E-O Le Bigot, Y-W Liu, J A M Lopes, L Ludhova, C M B Monteiro, F Mulhauser, T Nebel, F Nez, P Rabinowitz, J M F dos Santos, L A Schaller, K Schuhmann,

- C Schwob, D Taqqu, J F C A Veloso, and R Pohl. The proton radius puzzle. *Journal of Physics: Conference Series*, 312(3):032002, 2011.
- [42] Sungtae Cho et al. Multi-quark hadrons from Heavy Ion Collisions. *Phys. Rev. Lett.*, 106:212001, 2011.
- [43] Arthur M. Poskanzer and S. A. Voloshin. Methods for analyzing anisotropic flow in relativistic nuclear collisions. *Phys. Rev.*, C58:1671–1678, 1998.
- [44] Kai Xiao, Feng Liu, and Fuqiang Wang. Event-plane decorrelation over pseudo-rapidity and its effect on azimuthal anisotropy measurement in relativistic heavy-ion collisions. *Phys.Rev.*, C87:011901, 2013.
- [45] Jean-Yves Ollitrault. Determination of the reaction plane in ultrarelativistic nuclear collisions. *Phys. Rev.*, D48:1132–1139, 1993.
- [46] V. Borka Jovanovic, S. R. Ignjatovic, D. Borka, and P. Jovanovic. Constituent quark masses obtained from hadron masses with contributions of Fermi-Breit and Glozman-Riska hyperfine interactions. *Phys. Rev.*, D82:117501, 2010.